Protein Engineered Nanoscale Micelles for Dynamic ^{19}F Magnetic Resonance and Therapeutic Drug Delivery

Lindsay K. Hill[†,‡,§,¶,°], Joseph A. Frezzo[†,°], Priya Katyal[†], Dung Minh Hoang[‡,§], Zakia Ben Youss Gironda[‡,§], Cynthia Xu[†], Xuan Xie[†], Erika Delgado-Fukushima[†], Youssef Z. Wadghiri[‡,§,*], Jin Kim Montclare[†,§,‖,⊥,*]

†. Department of Chemical and Biomolecular Engineering, New York University Tandon School of Engineering, Brooklyn, New York, 11201, USA
‡. Center for Advanced Imaging Innovation and Research (CAI^{2}R), New York University School of Medicine, New York, New York, 10016, USA
§. Bernard and Irene Schwartz Center for Biomedical Imaging, Department of Radiology, New York University School of Medicine, New York, New York, 10016, USA
¶. Department of Biomedical Engineering, SUNY Downstate Medical Center, Brooklyn, New York, 11203, USA
‖. Department of Chemistry, New York University, New York, New York, 10012, USA
⊥. Department of Biomaterials, New York University College of Dentistry, New York, New York, 10010, USA
* Corresponding Authors
Email: Montclare@nyu.edu, Youssef.ZaimWadghiri@nyulangone.org
° These two authors contributed equally to this work

SUPPORTING INFORMATION

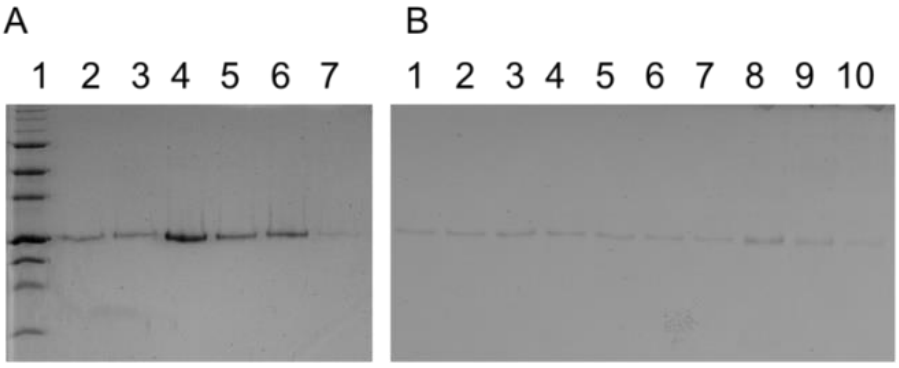

Figure S1. SDS-PAGE of post-purification protein elutions under increasing imidazole concentrations showing A) F-TRAP purity: 1- Ladder, 2- 100 mM, 3- 100 mM, 4- 150 mM, 5- 150 mM, 6- 300 mM, 7- 300 mM imidazole and B) TRAP purity: 1- 100 mM, 2- 100 mM, 3- 100 mM, 4- 150 mM, 5- 150 mM, 6- 300 mM, 7- 300 mM, 8- 500 mM, 9- 500 mM, 10-1000 mM imidazole.

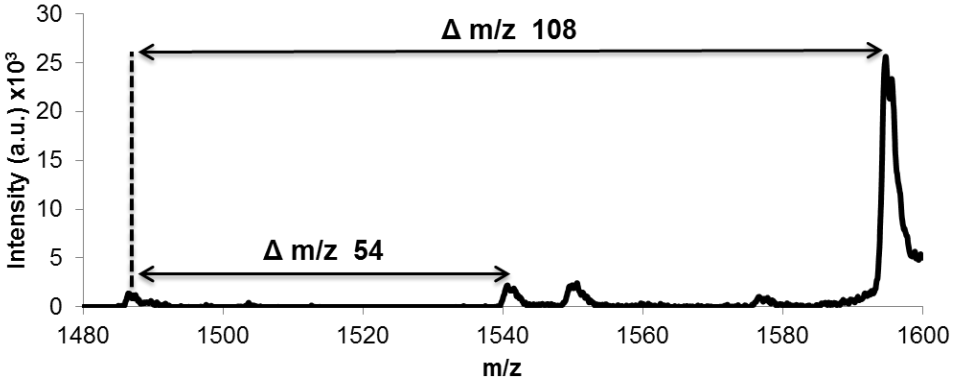

Figure S2. MALDI-TOF spectra of tryptic fragment $EL_{TFL}QETNAAL_{TFL}QDVR$.

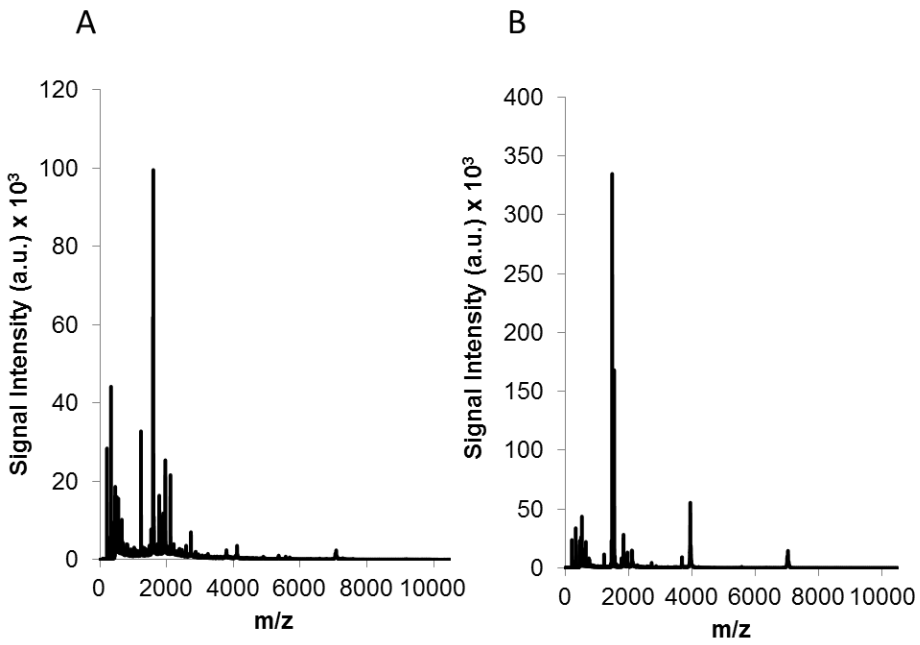

Figure S3. MALDI-TOF spectra of A) TRAP and B) F-TRAP.

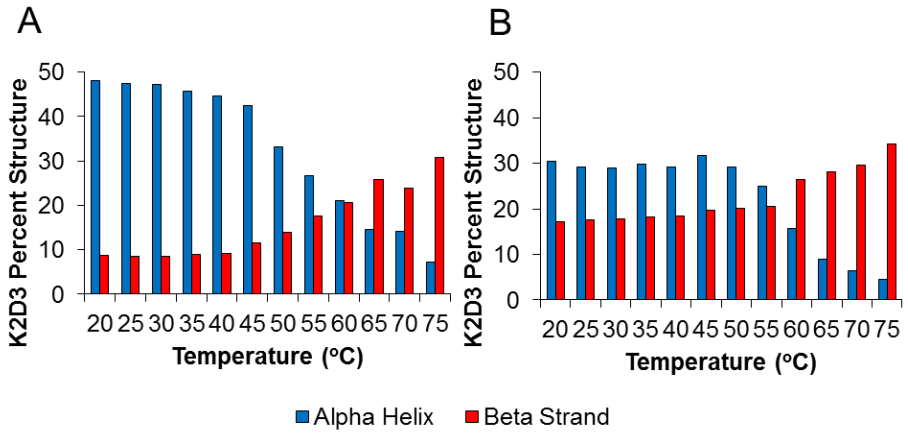

Figure S4. Secondary structure analysis of A) TRAP and B) F-TRAP as analyzed by K2D3 circular dichroism deconvolution software.

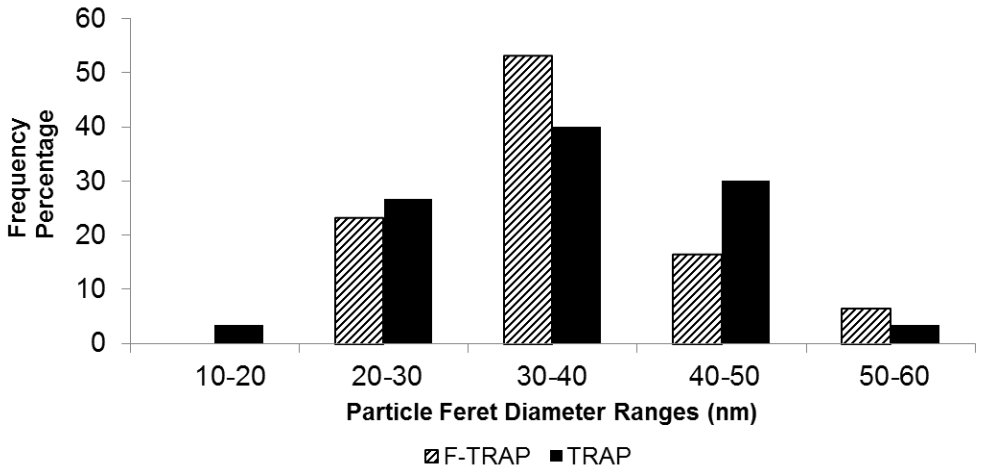

Figure S5. Frequency distribution of feret diameters for F-TRAP (hashed) and TRAP (solid) particles measured on transmission electron micrographs. Values measured using ImageJ.

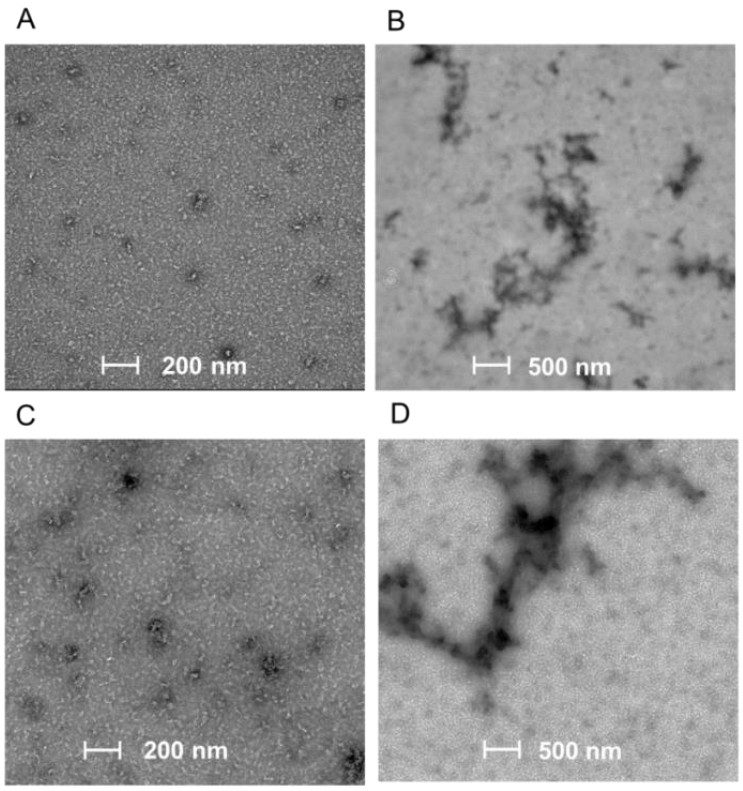

Figure S6. Transmission electron micrographs of F-TRAP at A) 20°C and B) 50°C, and TRAP at C) 20°C and D) 50°C.

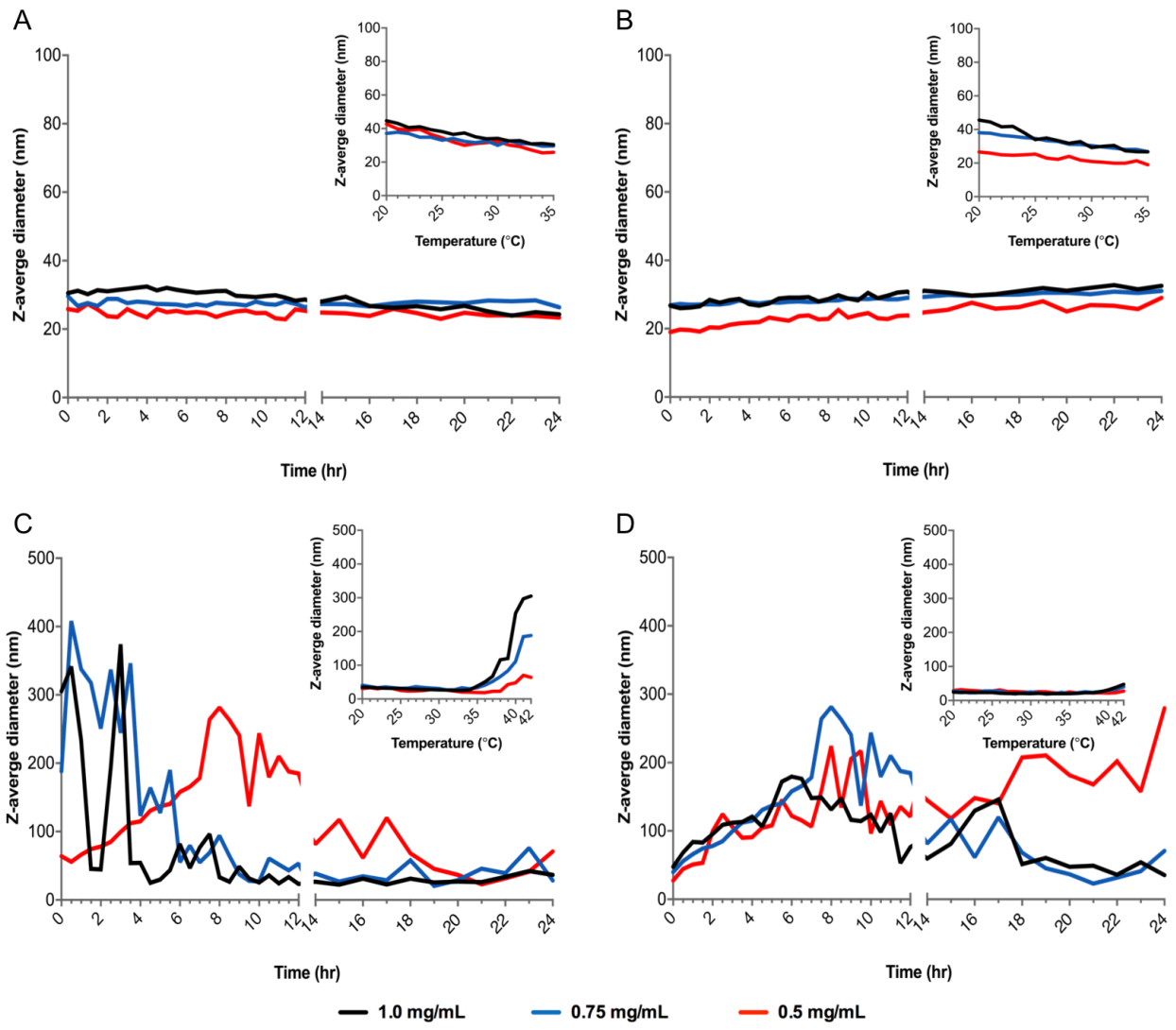

Figure S7. A) F-TRAP and B) TRAP diameters by DLS from 20°C to 35°C (inset) and held at 35°C for up to 24 hr. C) F-TRAP and D) TRAP diameters by DLS from 20°C to 42°C (inset) and held at 42°C for up to 24 hr.

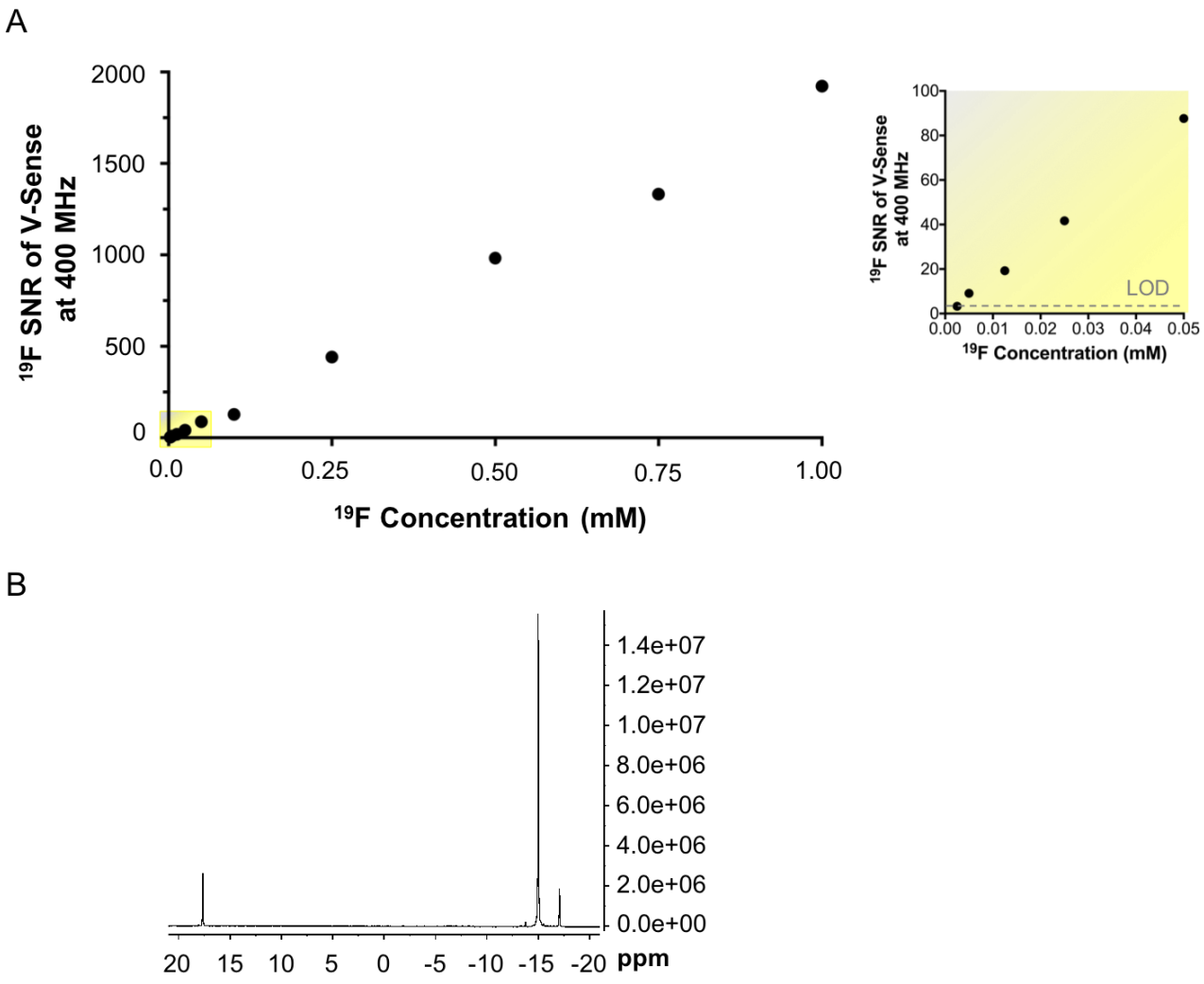

Figure S8. A) Signal-to-noise ratios (SNR) from one-dimensional ^{19}F NMR spectra of V-Sense diluted from 1.0 mM ^{19}F to its limit of detection (LOD), at which SNR=3,[1] of 0.0025 mM ^{19}F. Inset is focused on the lower ^{19}F concentrations to better show the LOD. B) Representative NMR spectra of V-Sense at 0.75 mM ^{19}F.

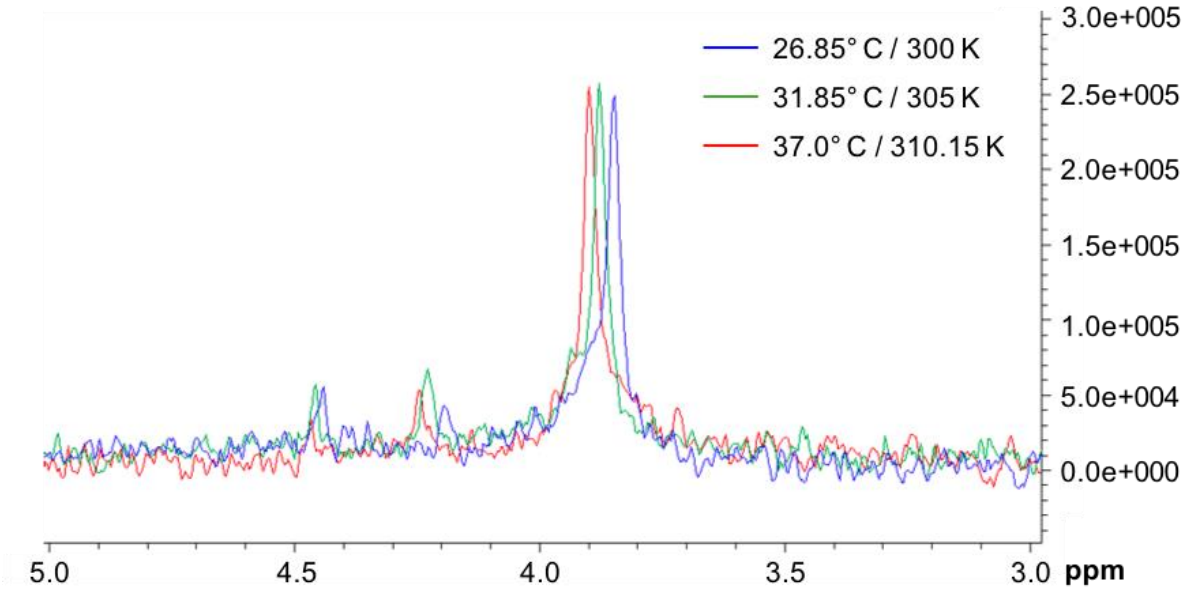

Figure S9. One-dimensional ^{19}F NMR spectra for F-TRAP (1.0 mg/mL, 1.63 mM ^{19}F) zoomed over a 2 ppm chemical shift window acquired at 400 MHz (9.4 Tesla) to show the three F-TRAP peaks acquired while increasing the temperature from 26.85 to 31.85 and 37.0°C, each calibrated to a 10% Trifluoroethanol/10% D_2O/80% H_2O standard acquired at the corresponding temperature. It must be noted that the < 1 ppm chemical shift spread covered by these three peaks translates into an absolute frequency excursion of 300 Hz at 7 Tesla (300 MHz). This three-peak frequency spread is more than half the receiver sweep width (SW) chosen for the ZTE sequence (SW=781 Hz/pixel) used to acquire the ^{19}F images shown in Figure S10. Importantly, this greater SW enables the integration of the signal from the three peaks into a single pixel while preventing chemical shift artifacts commonly seen in the frequency-encoding as spatially mis-registered pixels.

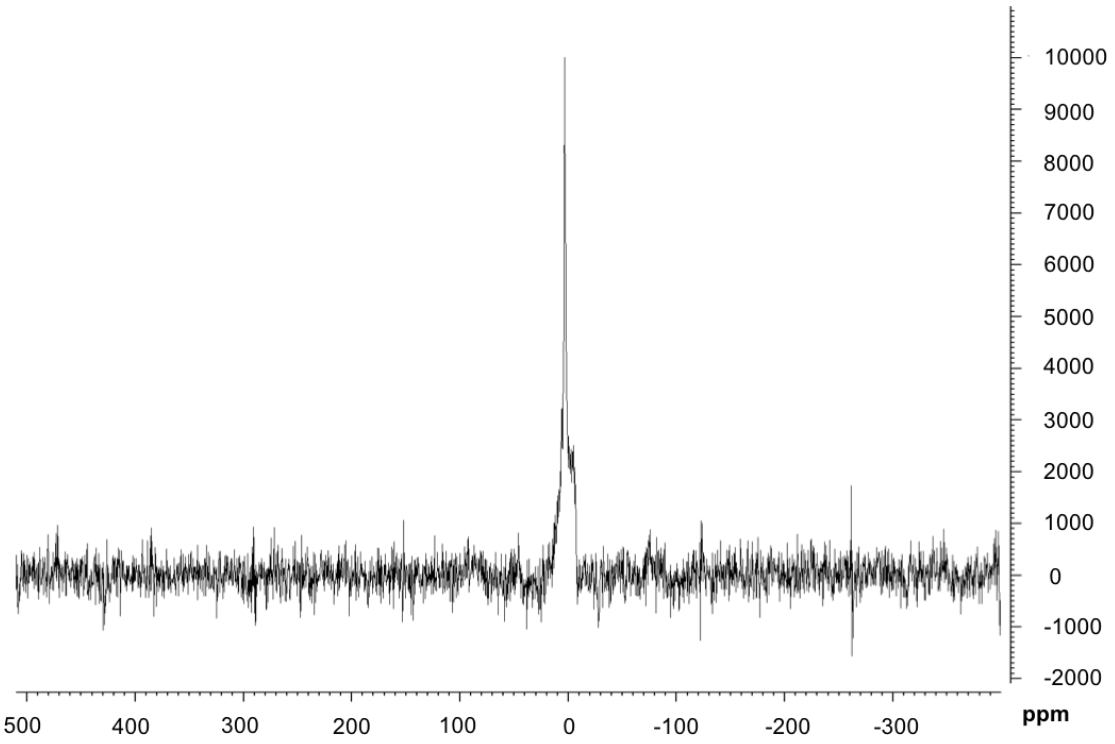

Figure S10. ^{19}F MRS of a phantom F-TRAP sample at 13.40 mg/mL or 0.82 mM protein, equivalent to 21.90 mM ^{19}F, acquired in 6 min 40 sec at 7 Tesla (300 MHz).

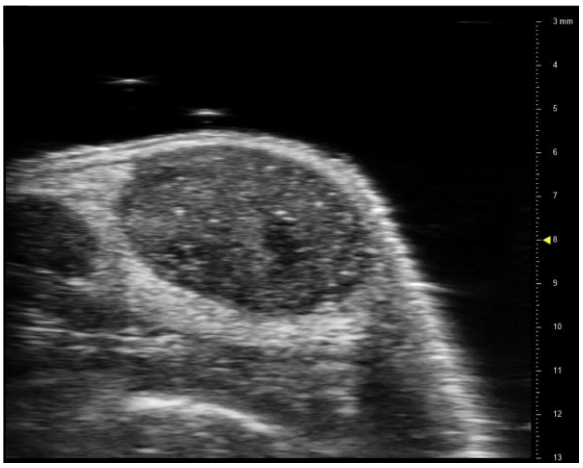

Figure S11. Example of a 2D high frequency ultrasound image showing the MCF-7 tumor mass implanted in an CrTac:NCr-*Foxn1*^{nu} mouse in order to rapidly assess the 3D tumor volume and perform real-time guided intratumoral injection of NIR-F-TRAP.

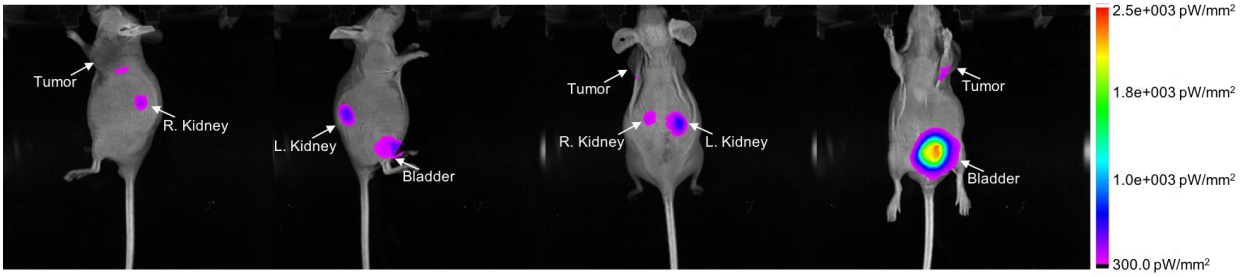

Figure S12. Example of *in vivo* dual multispectral VIS-NIR fluorescence and reflectance imaging, shown in four different orientations, using a bioluminescence and fluorescence scanner 24 hours following intratumoral injection of NIR-F-TRAP into an MCF-7 xenograft CrTac:NCr-*Foxn1*^{nu} mouse to qualitatively assess the pharmacokinetics and bioavailability of NIR-F-TRAP.

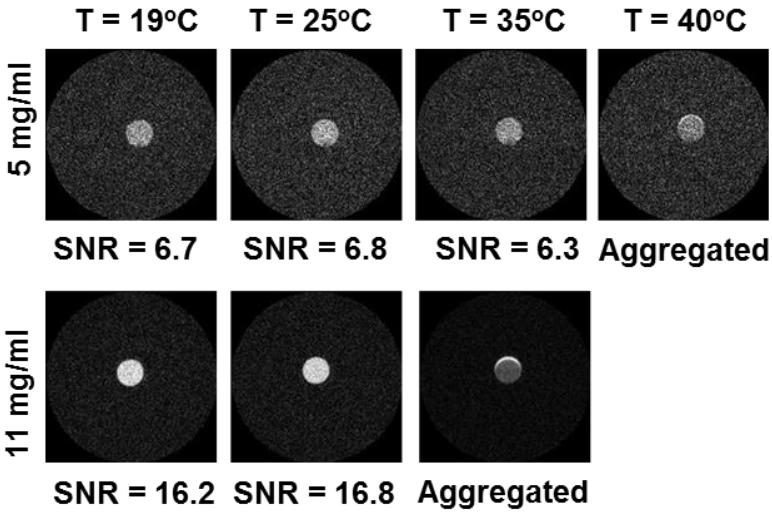

Figure S13. Temperature dependence of ^{19}F ZTE MRI of F-TRAP at 5 mg/mL (8.17 mM ^{19}F) and 11 mg/mL (17.98 mM ^{19}F) while increasing temperature. This study aimed at illustrating the reliability of the ZTE pulse sequence despite the dramatic shortening of the transverse T_2 relaxation times of F-TRAP associated with the temperature changes. Notwithstanding the large change in temperature of F-TRAP over a 16°C range, the SNR showed less than 6% deviation for both concentrations. Importantly, the MRI experiments echoed previous characterizations where increased concentration of F-TRAP is expected to lower the temperature of aggregation as depicted.

Table S1. Expression Yields[a] (mg/L) for F-TRAP and TRAP after recombinant expression in LAM 1000 *E. coli.*

F-TRAP	TRAP
29.17 ± 3.91	48.30 ± 6.43

[a] Yields are an average of three separate expressions under identical conditions

Table S2. Trifluoroleucine (TFL) incorporation levels as measured by Amino Acid Analysis (AAA) and MALDI-TOF MS Analysis.

	AAA	MALDI-TOF
TFL Incorporation (%)	81.36 ± 5.22%	80.90 ± 1.02%

Table S3. Mean residue ellipticity values and melting temperatures of F-TRAP and TRAP.

Protein	$-\theta_{208}$ (deg•cm^2•dmol^{-1})	$-\theta_{222}$ (deg•cm^2•dmol^{-1})	T_m (°C)
F-TRAP	-10615.40 ± 2955.19	-10270.90 ± 2753.07	59.3 ± 2.3
TRAP	-15458.43 ± 938.32	-14901.35 ± 1350.70	54.0 ± 2.0

Table S4. Inverse transition temperatures of F-TRAP and TRAP.

Conc. (mg/mL)	F-TRAP T_t (°C)	TRAP T_t (°C)
1.00	45.71 ± 0.51	41.60 ± 0.56
0.75	46.36 ± 0.03	42.48 ± 0.24
0.50	47.87 ± 0.72	44.16 ± 0.30
0.20	52.04 ± 0.84	47.32 ± 1.39

Table S5. F-TRAP particle z-average diameters measured by dynamic light scattering.

Temperature (°C)	0.5 mg/mL	0.75 mg/mL	1.0 mg/mL
20	30.30 ± 0.60	30.26 ± 0.81	30.83 ± 0.53
21	27.44 ± 1.26	29.97 ± 0.36	30.67 ± 0.15
22	28.27 ± 1.04	29.98 ± 0.68	29.87 ± 0.35
23	28.73 ± 1.32	29.31 ± 0.92	28.61 ± 0.76
24	27.07 ± 0.22	27.95 ± 0.08	28.39 ± 0.19
25	25.21 ± 1.07	27.95 ± 0.42	27.54 ± 0.13
26	26.16 ± 1.40	27.21 ± 0.42	27.64 ± 0.29
27	25.42 ± 0.76	26.42 ± 0.11	28.07 ± 0.39
28	23.19 ± 1.34	25.16 ± 0.07	27.60 ± 0.64
29	25.65 ± 0.51	25.12 ± 0.30	29.27 ± 0.67
30	24.04 ± 2.22	24.88 ± 0.89	29.37 ± 1.13
31	24.47 ± 0.37	24.19 ± 0.47	29.43 ± 0.35
32	24.16 ± 0.79	24.65 ± 0.49	30.85 ± 0.33
33	24.40 ± 1.21	24.74 ± 0.21	31.83 ± 1.55
34	20.96 ± 0.70	23.74 ± 0.15	33.70 ± 1.13
35	23.18 ± 1.25	24.05 ± 0.33	33.70 ± 0.64
36	22.83 ± 0.79	23.76 ± 0.46	34.98 ± 0.68
37	22.72 ± 0.13	25.04 ± 0.10	35.76 ± 0.98
38	22.37 ± 1.13	31.08 ± 1.74	36.00 ± 0.35
39	28.33 ± 1.20	35.87 ± 0.88	37.46 ± 0.28
40	42.32 ± 3.46	38.03 ± 0.76	41.06 ± 0.70

41	48.63 ± 0.87	40.70 ± 1.14	51.78 ± 5.67
42	48.62 ± 2.16	56.83 ± 1.36	73.75 ± 6.27
43	95.65 ± 44.54	79.80 ± 7.77	146.70 ± 48.91
44	187.30 ± 24.21	126.80 ± 38.20	470.30 ± 15.17
45	210.20 ± 56.53	321.70 ± 49.44	710.40 ± 20.38
46	329.20 ± 37.58	588.80 ± 59.10	831.80 ± 38.19
47	486.70 ± 48.17	712.80 ± 55.82	868.90 ± 58.57
48	546.70 ± 20.40	750.50 ± 62.01	879.60 ± 105.90
49	589.20 ± 18.15	819.40 ± 43.95	901.80 ± 107.60
50	688.90 ± 31.74	888.30 ± 93.30	1279.00 ± 205.20

Table S6. TRAP particle z-average diameters measured by dynamic light scattering.

Temperature (°C)	0.5 mg/mL	0.75 mg/mL	1.0 mg/mL
20	32.14 ± 1.20	30.81 ± 0.39	31.93 ± 0.22
21	31.23 ± 0.40	30.16 ± 0.33	31.38 ± 0.39
22	30.18 ± 0.50	29.97 ± 0.18	30.61 ± 0.34
23	29.35 ± 0.77	29.66 ± 0.26	29.91 ± 0.74
24	28.76 ± 0.31	28.83 ± 0.70	29.89 ± 0.33
25	28.65 ± 0.52	28.40 ± 0.74	29.65 ± 0.26
26	28.81 ± 0.16	28.17 ± 0.22	30.01 ± 0.45
27	28.64 ± 0.54	29.15 ± 0.42	29.50 ± 0.34
28	29.21 ± 0.56	28.87 ± 0.17	31.07 ± 0.26
29	29.41 ± 1.20	30.78 ± 0.54	31.35 ± 0.66
30	29.12 ± 0.73	30.35 ± 0.96	31.92 ± 0.10
31	29.01 ± 0.49	31.06 ± 1.91	31.93 ± 0.23
32	29.40 ± 1.08	31.74 ± 0.24	33.12 ± 0.51
33	29.91 ± 1.12	32.28 ± 0.50	31.88 ± 0.41
34	30.30 ± 1.01	31.91 ± 1.31	31.75 ± 2.42
35	30.21 ± 1.24	32.74 ± 0.84	28.53 ± 0.70
36	29.65 ± 0.34	30.50 ± 1.38	29.38 ± 0.51
37	31.05 ± 0.86	30.02 ± 1.01	31.26 ± 0.70
38	32.64 ± 0.31	30.67 ± 1.55	32.70 ± 0.48
39	33.95 ± 0.12	33.36 ± 0.99	34.29 ± 1.07

40	35.79 ± 1.28	40.84 ± 4.86	63.72 ± 6.33
41	56.53 ± 8.57	95.24 ± 11.48	185.40 ± 42.30
42	177.50 ± 25.33	396.20 ± 21.20	818.20 ± 103.20
43	408.30 ± 25.45	602.10 ± 37.48	1175.00 ± 84.89
44	578.00 ± 56.19	694.70 ± 62.50	1399.00 ± 199.50
45	669.20 ± 84.52	777.30 ± 45.80	1533.00 ± 215.60
46	724.40 ± 70.68	783.50 ± 52.52	1681.00 ± 398.80
47	747.90 ± 42.48	761.10 ± 55.40	1835.00 ± 217.10
48	771.10 ± 43.12	779.10 ± 70.24	1320.00 ± 209.80
49	817.50 ± 20.62	955.00 ± 208.70	1973.00 ± 802.40
50	823.90 ± 72.82	1676.00 ± 438.00	2648.00 ± 1352.00

Table S7. F-TRAP particle measurements by transmission electron microscopy. Protein samples were incubated at 20°C and 0.5 mg/mL prior to spotting, and particles were measured using ImageJ.

Particle No.	Area (nm^2)	Perimeter (nm)	Feret Diameter (nm)	Circularity
1	608	109.207	39.446	0.640637155
2	324	73.351	26.907	0.756732575
3	500	86.517	32.802	0.839414753
4	300	65.677	25.612	0.873985321
5	575	90.657	33.526	0.879173634
6	315.75	79.018	27.785	0.635478395
7	366.5	80.826	34.409	0.704987316
8	480.5	86.319	34.000	0.810382564
9	410.5	76.012	31.241	0.892808547
10	415	80.319	32.558	0.808390141
11	501	100.939	35.384	0.617915696
12	523	94.221	32.558	0.740313668
13	441	81.513	32.802	0.834054313
14	566.5	93.073	32.802	0.821792146
15	240	68.441	25.298	0.64385496
16	434.5	84.03	32.802	0.773268913
17	432	80.623	31.623	0.835170865
18	483.5	101.161	41.231	0.59371736
19	374.5	77.781	30.529	0.777882989
20	324	66.538	24.413	0.919634006

21	644.5	115.314	41.231	0.609071593
22	409.5	82.548	32.249	0.755179674
23	751	123.438	48.332	0.619372161
24	669.5	102.861	41.037	0.79516745
25	892.5	119.235	48.374	0.788878663
26	597.5	110.603	36.056	0.613781216
27	587	95.856	31.241	0.802803013
28	1234.75	152.049	60.926	0.671152783
29	1269	166.074	56.321	0.57818634
30	481	81.9	29.732	0.901128593

Table S8. TRAP particle measurements by transmission electron microscopy. Protein samples were incubated at 20°C and 0.5 mg/mL prior to spotting, and particles were measured using ImageJ.

Particle No.	Area (nm^2)	Perimeter (nm)	Feret Diameter (nm)	Circularity
1	399.434	88.41	32.311	0.642173
2	418.104	93.133	31.759	0.605741
3	412.7	81.26	26.965	0.785399
4	1209.603	140.712	44.958	0.767697
5	515.875	122.616	46.685	0.431181
6	210.28	56.885	19.85	0.816605
7	679.481	141.755	43.548	0.424923
8	389.608	78.873	25.408	0.787011
9	807.712	110.456	42.382	0.831931
10	537.492	97.465	33.063	0.711024
11	822.943	141.299	44.137	0.517966
12	383.221	75.419	29.944	0.846637
13	1093.163	130.088	46.758	0.811746
14	782.164	108.17	41.039	0.840028
15	434.809	90.864	36.354	0.661796
16	407.787	97.997	36.042	0.533602
17	455.935	90.313	33.936	0.702444
18	574.341	92.54	33.322	0.842792
19	304.12	78.891	26.01	0.614044
20	310.999	74.796	27.914	0.698573

21	288.399	69.97	26.339	0.740252
22	626.911	103.246	36.99	0.739042
23	301.173	84.23	31.697	0.533448
24	550.266	109.68	38.577	0.574814
25	160.658	52.48	20.072	0.733034
26	566.48	128.947	45.491	0.428126
27	464.779	98.45	35.444	0.602594
28	521.77	97.256	33.241	0.693196
29	197.015	78.502	28.601	0.401742
30	607.75	120.476	50.355	0.526179

Table S9. Doxorubicin loading efficiencies and weighted loading amounts for F-TRAP and TRAP.

Protein	Loading Efficiency (%) (Total recovered Doxorubicin in protein)	Weighted Loading (µg Doxorubicin/ mg protein)
F-TRAP	49.10	29.90 ± 2.68
TRAP	17.80	19.22 ± 2.19

Table S10. ^{19}F R_1 relaxometry values as a function of concentration and temperature.

	R_1 ($1/T_1$) msec^{-1}			
	Temperature (°C)			
Concentration (mg/mL)	**22**	**27**	**32**	**37**
0.50	0.0040348	0.00270446	0.002594862	0.00256192
0.60	0.00259622	0.00249556	0.002279176	0.0021438
0.75	0.00221131	0.00214099	0.001976	0.00179558
0.90	0.00254573	0.00243374	0.002244649	0.00214064

Table S11. ^{19}F R_2 Relaxometry values as a function of concentration and temperature.

	R_2 ($1/T_2$) msec^{-1}			
	Temperature (°C)			
Concentration (mg/mL)	**22**	**27**	**32**	**37**
0.50	0.45372051	1.18743551	2.40390972	3.08211051
0.60	0.99502488	2.23005218	4.79002908	6.29683269
0.75	1.23986104	2.44156123	4.64787685	7.45311988
0.90	0.84175084	2.58797832	4.64699131	8.30288941

REFERENCE

(1) Shrivastava, A.; Gupta, V. Methods for the Determination of Limit of Detection and Limit of Quantitation of the Analytical Methods. *Chron. Young Sci.* **2011**, *2*, 21–25.